

Breviscapine Pretreatment Inhibits Myocardial Inflammation and Apoptosis in Rats After Coronary Microembolization by Activating the PI3K/Akt/GSK-3 β Signaling Pathway

This article was published in the following Dove Press journal:
Drug Design, Development and Therapy

Zhi-Qing Chen¹
You Zhou¹ 
Feng Chen²
Jun-Wen Huang¹
Jing Zheng¹
Hao-Liang Li¹
Tao Li¹
Lang Li¹

¹Department of Cardiology, The First Affiliated Hospital of Guangxi Medical University & Guangxi Key Laboratory Base of Precision Medicine in Cardio-Cerebrovascular Diseases Control and Prevention & Guangxi Clinical Research Center for Cardio-Cerebrovascular Diseases, Nanning, People's Republic of China; ²Department of Emergency, The First Affiliated Hospital of Guangxi Medical University, Nanning, People's Republic of China

Correspondence: Lang Li
Department of Cardiology, The First Affiliated Hospital of Guangxi Medical University & Guangxi Key Laboratory Base of Precision Medicine in Cardio-Cerebrovascular Diseases Control and Prevention & Guangxi Clinical Research Center for Cardio-Cerebrovascular Diseases, 6 Shuangyong Road, Nanning, 530021, Guangxi, People's Republic of China
Tel/Fax +86-771-5331171
Email drililang99@126.com

Purpose: Coronary microembolization (CME) can cause myocardial inflammation, apoptosis and progressive cardiac dysfunction. On the other hand, breviscapine exerts a significant cardioprotective effect in many cardiac diseases although its role and the potential mechanisms in CME remain unclear. Therefore, the present study aimed to ascertain whether pretreatment with breviscapine could improve CME-induced myocardial injury by alleviating myocardial inflammation and apoptosis. The possible underlying mechanisms were also explored.

Methods: In this study, 48 Sprague-Dawley (SD) rats were randomly assigned to the CME, CME + breviscapine (CME + BE), CME + breviscapine + LY294002 (CME + BE + LY) and sham groups (12 rats per group). In addition, the CME model was successfully established by injecting 42 μ m inert plastic microspheres into the left ventricle of rats. Rats in the CME + BE and CME + BE + LY groups received 40 mg/kg/d of breviscapine for 7 days before inducing CME. Moreover, rats in the CME + BE + LY group were intraperitoneally injected with the phosphoinositide 3-kinase (PI3K) specific inhibitor, LY294002 (10 mg/kg) 30 minutes before CME modeling. 12 h after surgery, the study measured cardiac function, the serum levels of markers of myocardial injury, myocardial inflammation-associated mRNAs and proteins, myocardial apoptosis-associated mRNAs and proteins and conducted myocardial histopathology.

Results: The findings demonstrated that pretreatment with breviscapine alleviated myocardial injury following CME by improving cardiac dysfunction, decreasing the serum levels of markers of myocardial injury, reducing the size of myocardial microinfarct and lowering the cardiomyocyte apoptotic index. More importantly, pretreatment with breviscapine resulted to a decrease in the levels of inflammatory and pro-apoptotic mRNAs and proteins in myocardial tissues and there was an increase in the levels of anti-apoptotic mRNAs and proteins. However, these protective effects were eliminated when breviscapine was combined with LY294002.

Conclusion: The findings from this study indicated that breviscapine may inhibit myocardial inflammation and apoptosis by regulating the PI3K/protein kinase B (Akt)/glycogen synthase kinase-3 β (GSK-3 β) pathway, thereby ameliorating CME-induced cardiac dysfunction and reducing myocardial injury.

Keywords: breviscapine, coronary microembolization, PI3K/Akt/GSK-3 β , myocardial inflammation, apoptosis

Introduction

Coronary microembolization (CME) can lead to slow or even lack of reflow in the myocardium and occurs due to percutaneous coronary intervention (PCI) for acute

coronary syndrome or spontaneous rupture of an atherosclerotic plaque. This can in turn result to regional myocardial systolic dysfunction and fatal arrhythmia. In addition, CME is well recognized as a strong and independent predictor of long-term adverse prognosis and major adverse cardiac events in patients.^{1,2} Previous studies showed that the area of myocardial micro-infarction is accompanied by a large number of inflammatory cell infiltration and necrotic/apoptotic cardiomyocytes following CME. This plays a crucial role in CME-induced myocardial injury and progressive cardiac dysfunction. Therefore, inhibition of myocardial inflammation and apoptosis can distinctly improve cardiac function and myocardial injury.^{3,4} Moreover, studies by Liang et al⁵ and Kong et al⁶ demonstrated that myocardial apoptosis and inflammation can induce heart dysfunction and myocardial injury, after CME in rats. However, pretreatment with ligustrazine significantly reduced myocardial apoptosis and inflammation induced by CME, thus relieving myocardial injury and ameliorating cardiac contractile function by activating the phosphoinositide 3-kinase (PI3K)/protein kinase B (Akt) pathway.⁷

Breviscapine is mainly extracted from the traditional Chinese herb *Erigeron breviscapus* and contains scutellarin (4',5,6-tetrahydroxyflavone-7-O-glucuronide) as the major active component.⁸ Interestingly, breviscapine is characterized by extensive pharmacological activity, high safety and few side effects. In addition, recent findings on cardiovascular diseases confirmed that breviscapine played numerous cardioprotective roles, including anti-inflammatory,⁹ anti-oxidative stress,¹⁰ anti-apoptosis¹¹ and improvement of left ventricular remodeling.¹² However, little information exists on the cardioprotective effects and potential molecular mechanisms of breviscapine in the management of CME-induced myocardial inflammation and apoptosis. Moreover, breviscapine was shown to effectively suppress inflammation by reducing the levels of serum tumor necrosis factor- α (TNF- α), interleukin-6 (IL-6) and interleukin-18 (IL-18).¹³ An additional study by Wang et al¹⁴ also revealed that breviscapine can distinctly inhibit cardiomyocyte apoptosis by activating the PI3K/Akt/endothelial nitric oxide synthase (eNOS) pathway. However, there is still a lack of relevant research that simultaneously explores the effect of breviscapine on myocardial inflammation and apoptosis in the same animal model of cardiovascular disease. Consequently, the present study sought to ascertain whether treatment with breviscapine had an effect on CME-induced myocardial

inflammation and apoptosis by activating the PI3K/Akt/glycogen synthase kinase-3 β (GSK-3 β) signaling pathway.

Materials and Methods

Animal Preparation

Approval to use the animals was obtained from the Clinical and Animal Research Ethics Committee of Guangxi Medical University and all the procedures conformed to the National Institute of Health Guidelines on the Use of Laboratory Animals. Consequently, 48 healthy (male, 250–300g) 8-week-old Sprague Dawley (SD) rats were purchased from the Experimental Animal Center of Guangxi Medical University. All the rats were then housed in a room where standard tap water and rat food were available. In addition, the temperature was maintained at $23 \pm 2^\circ\text{C}$ while humidity was controlled at 50–60% and the light/dark cycle was maintained at 12 h dark: 12 h light.

Grouping and Establishment of the CME Model

The 48 SD rats were stochastically assigned into four groups of 12 individuals each, namely, sham, CME, CME + breviscapine (CME + BE) and CME + breviscapine + LY294002 (CME + BE + LY). In particular, rats in the CME + BE and CME + BE + LY groups received breviscapine (Baishan Pharmaceutical Co., Ltd, Hebei, China) at a dose of 40 mg/kg daily by gavage, for 7 days before inducing CME. The dose and duration of breviscapine were based on previous studies by Zhong et al¹⁵ and Yan et al.⁹ On the other hand, rats in the CME+BE+LY group were intraperitoneally injected with LY294002 (APEX BIO, Houston, USA) at a dose of 10 mg/kg, 30 minutes before the CME surgery. Following a previously published protocol by Mao et al¹⁶ 30–40 mg/kg of pentobarbital sodium was used to anaesthetize the rats through the intraperitoneal route. The animals were then intubated and ventilated using a small animal ventilator to facilitate aerobic respiration. Thereafter, a thoracotomy was performed in the third and fourth intercostal space at the left edge of the sternum. Following this, the ascending aorta was fully separated and exposed after which it was clamped with a vascular clamp for 10 s. Three thousand polyethylene microspheres (BioSphere Medical Inc., Rockland, USA) with a diameter of 42 μm and suspended in 0.1 mL of physiological saline, were simultaneously but rapidly injected into the cardiac apex of rats in the CME, CME + BE and CME + BE + LY groups. Thereafter, the

chest was sutured carefully and the endotracheal tube was removed after a normal heart rate and breathing returned. 800,000 IU of penicillin was subsequently injected intraperitoneally. Notably, rats in the sham group underwent the same surgical and experimental procedures although they were given physiological saline (0.1 mL) instead of microspheres. Finally, all the rats in the four groups were sacrificed 12 h after the operation.

Evaluation of Rat Cardiac Function

According to previous studies, cardiac function in experimental rats is usually at its worst, 12 h after CME modeling.¹⁷ Therefore, the present study assessed cardiac function at the same time point. Herein, the left ventricular ejection fraction (LVEF), left ventricular fractional shortening (LVFS), left ventricular end-diastolic diameter (LVEDd) and left ventricular end-systolic diameter (LVESd) were measured using the Hewlett Packard Sonos 7500 ultrasound instrument (Philips Technologies, USA) equipped with a 12 MHz transducer. In addition, an average of 3 cardiac cycles was applied to the above parameters and the echocardiographic measurements were independently taken by an expert.

Measurement of Serum Myocardial Injury Markers

Blood samples were obtained from the femoral vein of rats in each group, 12 h after CME induction or sham operation, prior to sacrifice. The study then used a commercial enzyme-linked immunosorbent assay (ELISA) kit (Bio-Swamp Biological Technology Co., Ltd, Wuhan, China) to measure the levels of serum cardiac troponin I (cTnI), according to the manufacturer's instructions. Additionally, an automatic biochemical analyzer (Olympus5400, Olympus Ltd. Japan) was used to detect the levels of lactate dehydrogenase (LDH) and the creatine kinase myocardial band isoenzyme (CK-MB).

Tissue Collection and Sample Processing

In order to collect myocardial tissue samples, 10% potassium chloride (2.0 mL) was injected into the caudal vein of rats in each group to isolate and harvest the heart immediately, while in diastole. Both the atria and atrial appendages were removed after which the left ventricle was divided into the apical and basal parts parallel to the atrioventricular groove at the midpoint of the left

ventricular long axis. Thereafter, the apical part of rats in each group was rapidly frozen with liquid nitrogen then transferred and stored at -80°C for the Western blot and quantitative real-time polymerase chain reaction (qRT-PCR) analyses. On the other hand, the basal tissue of the heart was fixed for about 12 h in 4% paraformaldehyde at room temperature, followed by embedding in paraffin and serial slicing into 4 μm thick sections, for subsequent staining using hematoxylin-eosin (H&E), hematoxylin-basic fuchsin-picric acid (HBFP), TdT-mediated dUTP nick end labeling (TUNEL) and immunohistochemistry (IHC).

Measurement of Myocardial Microinfarct Size

HBFP staining is generally considered as an important staining method during the early stage diagnosis of myocardial ischemia. After staining with HBFP, both ischemic cardiomyocytes and erythrocytes were dyed red while the cytoplasm and nucleus of normal cardiomyocytes stained yellow and blue, respectively. The study used a pathology image analyzer, DMR + Q550 (Leica, Wetzlar, Germany) to examine and analyze the HBFP-stained sections under a light microscope ($\times 100$ magnification). Additionally, five visual fields were randomly selected from each section using the Leica Qwin analysis software and the myocardial infarction zone was measured through the planar area method. Finally, the relative ischemic area (as a percentage) was calculated according to the following formula: $\text{ischemic area}/\text{total area} \times 100\%$.¹⁸

Detection of Myocardial Apoptosis Through TUNEL Staining

In order to determine the apoptotic index, the study conducted a quantitative analysis of cardiomyocyte apoptosis using the TUNEL apoptosis detection kit (Roche, USA) following the manufacturer's guidelines. In this staining method, the nuclei of normal cells in myocardial tissues appeared light blue while apoptotic cells stained yellow-brown (TUNEL-positive). Furthermore, the number of apoptotic cardiomyocytes and total cardiomyocytes in micro-infarcted, marginal infarcted and distal non-infarcted zones were counted from 5 randomly selected fields ($\times 400$ magnification) in each slice. Finally, the myocardial apoptotic rate was determined using the following formula: $\text{apoptotic cardiomyocytes}/\text{total cardiomyocytes} \times 100\%$.¹⁹

Quantitative Real-Time PCR (qRT-PCR)

Total RNA was extracted from the heart tissue using the TRIzol reagent (Invitrogen, USA) according to the manufacturer's instructions after which the concentration was measured using the NanoDrop (Thermo Fisher Scientific Inc., USA). Thereafter, the PrimeScript™ RT reagent Kit with a gDNA Eraser (Perfect Real Time) (TaKaRa, Japan) was used to reverse transcribe mRNA into complementary DNA. In addition, qRT-PCR was performed on the ABI PRISM 7500 system (CA, USA) using the TB Green® Premix Ex Taq™ II (Tli RNaseH Plus) (TaKaRa, Japan). The $2^{-\Delta\Delta C_t}$ method was then used to calculate the relative expression levels of the target genes and glyceraldehyde-3-phosphate dehydrogenase (GAPDH) was employed as an endogenous control. All primer sequences (TaKaRa, Japan) are shown in Table 1.

Western Blot Analysis

The total protein in each heart sample was extracted using a lysis buffer and the concentration was measured using a bicinchoninic acid (BCA) assay kit (PC0020, Beijing Solarbio Science & Technology Co., Ltd, Beijing, China). After determining the concentration, proteins of equal quality were separated using 10–15% sodium dodecyl sulphate-polyacrylamide gel electrophoresis (SDS-PAGE) before being electrophoretically transferred onto polyvinylidene fluoride (PVDF) membranes (Millipore, Atlanta, GA, USA). Thereafter, they were sealed for 1

h at room temperature in 5% bovine serum albumin or nonfat milk before being incubated overnight with the following primary antibodies (1: 1000 dilution) at 4°C: total PI3K, phospho-PI3K (p-PI3K), total Akt, phospho-Akt (p-Akt), total GSK-3β, phospho-GSK-3β (p-GSK-3β), TNF-α, IL-1β, cleaved caspase-3, Bcl-2, Bax or GAPDH. In addition, the primary antibodies specific to total PI3K, p-PI3K, TNF-α, IL-1β, Bax and Bcl-2 were provided by Abcam (Cambridge, UK). On the other hand, the primary antibodies specific to total Akt, p-Akt, total GSK-3β, p-GSK-3β, cleaved caspase-3 and GAPDH were supplied by Cell Signaling Technology (Beverly, USA). After overnight incubation, the membranes were washed 5 times with a 1×TBST buffer solution at room temperature and subsequently incubated with secondary antibodies labeled with horseradish peroxidase, for 2 h. Finally, the protein band of rats in each group was detected using an enhanced chemiluminescence detection system (Pierce, Rockford, IL, USA) and the expression levels were evaluated using the ImageJ software (National Institutes of Health, Bethesda, MD, USA).

Statistical Analysis

Statistical analyses were performed using the SPSS version 23.0 software (IBM, Chicago, USA) and the data was expressed as mean ± standard deviation (SD). In addition, statistical comparisons between two groups were conducted using the Student's *t*-test while multiple-group comparisons were performed using One-way Analysis of Variance (ANOVA) followed by the Student-Newman-Keuls posthoc analysis. A *p* value < 0.05 was considered to be statistically significant.

Results

Breviscapine Ameliorated Cardiac Function Following CME

The echocardiographic findings from rats in each group are indicated in Figure 1. The results revealed that cardiac contractility was impaired in the CME group, as indicated by increased LVESd and LVEDd but reduced LVEF and LVFS (*P* < 0.05), compared to the sham group. On the other hand, treatment with breviscapine significantly improved heart dysfunction, evidenced by lower LVESd and LVEDd values but higher LVEF and LVFS in the CME+BE group, compared to the CME group (*P* < 0.05). However, treatment with LY294002 eliminated the cardioprotective effects induced by breviscapine.

Table 1 Primer Sequence

Gene	Primer Sequence
TNF-α	Forward: 5'-CGTCGTAGCAAACCACCAAG-3' Reverse: 5'-GAGGCTGACTTTCTCCTGGT-3'
IL-1β	Forward: 5'-GGGATGATGACGACCTGCTA-3' Reverse: 5'-TGTCGTTGCTTGCTCTCCT-3'
Bcl-2	Forward: 5'-CCTGGCATCTTCTCCTTCCA-3' Reverse: 5'-GGACATCTCTGCAAAGTCGC-3'
Bax	Forward: 5'-AAGAAGCTGAGCGAGTGTCT-3' Reverse: 5'-CCAGTTGAAGTTGCCGTCTG-3'
Caspase-3	Forward: 5'-TGTCGATGCAGCTAACCTCA-3' Reverse: 5'-GCAGTAGTCGCCTCTGAAGA-3'
GAPDH	Forward: 5'-TGTGAACGGATTTGCCGTA-3' Reverse: 5'-GATGGTGTGGGTTTCCCGT-3'

Abbreviations: TNF-α, tumor necrosis factor-α; IL-1β, interleukin-1β; GAPDH, glyceraldehyde-3-phosphate dehydrogenase.

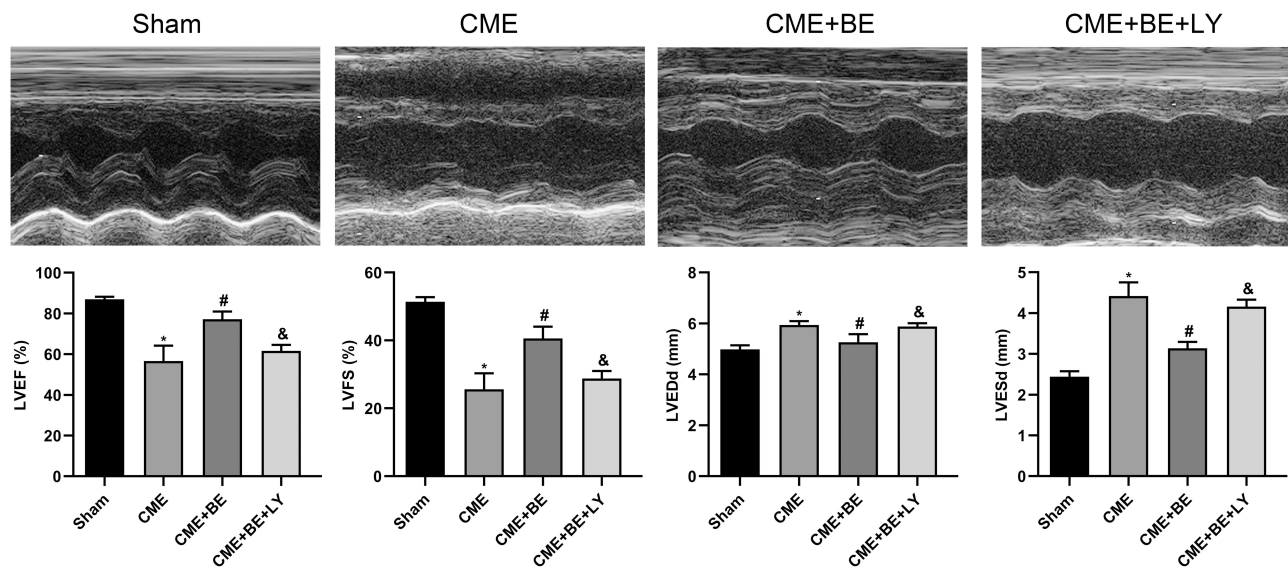


Figure 1 Echocardiography of rats in each group ($n = 5$ for each group). The cardiac function parameters of left ventricle ejection fraction (LVEF), left ventricle fractional shortening (LVFS), left ventricular end-diastolic diameter (LVEDd) and left ventricular end-systolic diameter (LVESd) were measured quantitatively. Data are presented as the mean \pm standard deviation (SD). * $P < 0.05$ versus the sham group; # $P < 0.05$ versus the CME group; & $P < 0.05$ versus the CME + BE group.

Abbreviations: CME, coronary microembolization; BE, breviscapine; LY, LY294002.

Breviscapine Reduced the Serum Levels of Myocardial Injury Markers

Myocardial injury following CME induction was assessed through the serum levels of cTnI, LDH and CK-MB (Figure 2). The results showed that rats from the CME group had significantly higher serum levels of cTnI, LDH and CK-MB compared to those in the sham group. In contrast, pretreatment with breviscapine significantly attenuated myocardial injury after CME, demonstrated by decreased levels of serum cTnI, LDH and CK-MB in the CME + BE group compared to the CME group. However,

treatment with a combination of breviscapine and LY294002 eliminated the effects of breviscapine on the expression levels of serum cTnI, LDH and CK-MB.

CME Histopathology

H&E and HBFP staining (Figure 3A and B) revealed sporadic subendocardial ischemia without noticeable infarction in the sham group although multiple microinfarctions were observed in the CME, CME + BE and CME + BE + LY groups. In addition, H&E staining showed that the nuclei of cardiomyocytes dissolved or disappeared in

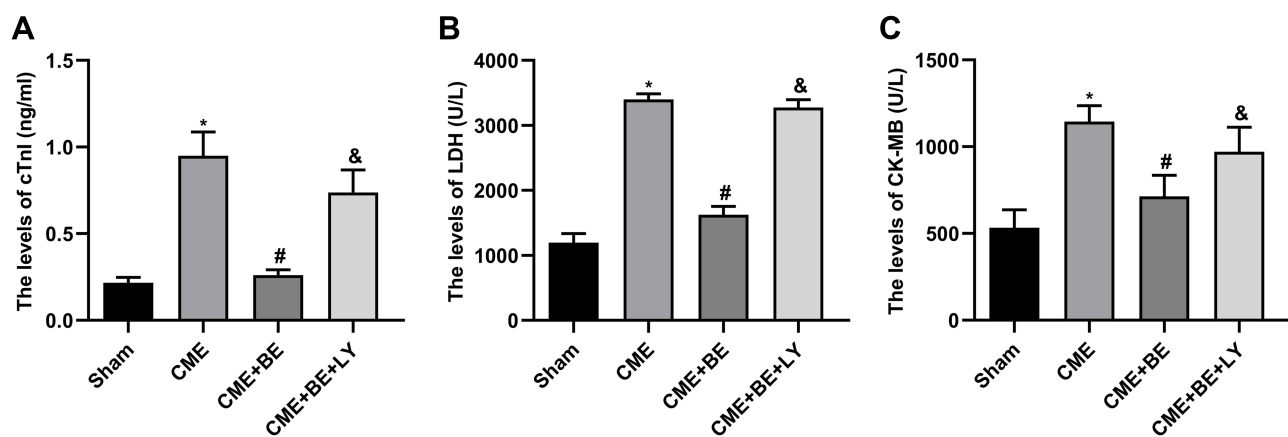


Figure 2 Breviscapine reduced the serum levels of markers of myocardial injury ($n = 4$ for each group). (A) The levels of cTnI in the four groups. (B) The levels of LDH in the four groups. (C) The levels of CK-MB in the four groups. Data are presented as the mean \pm standard deviation (SD). * $P < 0.05$ versus the sham group; # $P < 0.05$ versus the CME group; & $P < 0.05$ versus the CME + BE group.

Abbreviations: CME, coronary microembolization; BE, breviscapine; LY, LY294002.

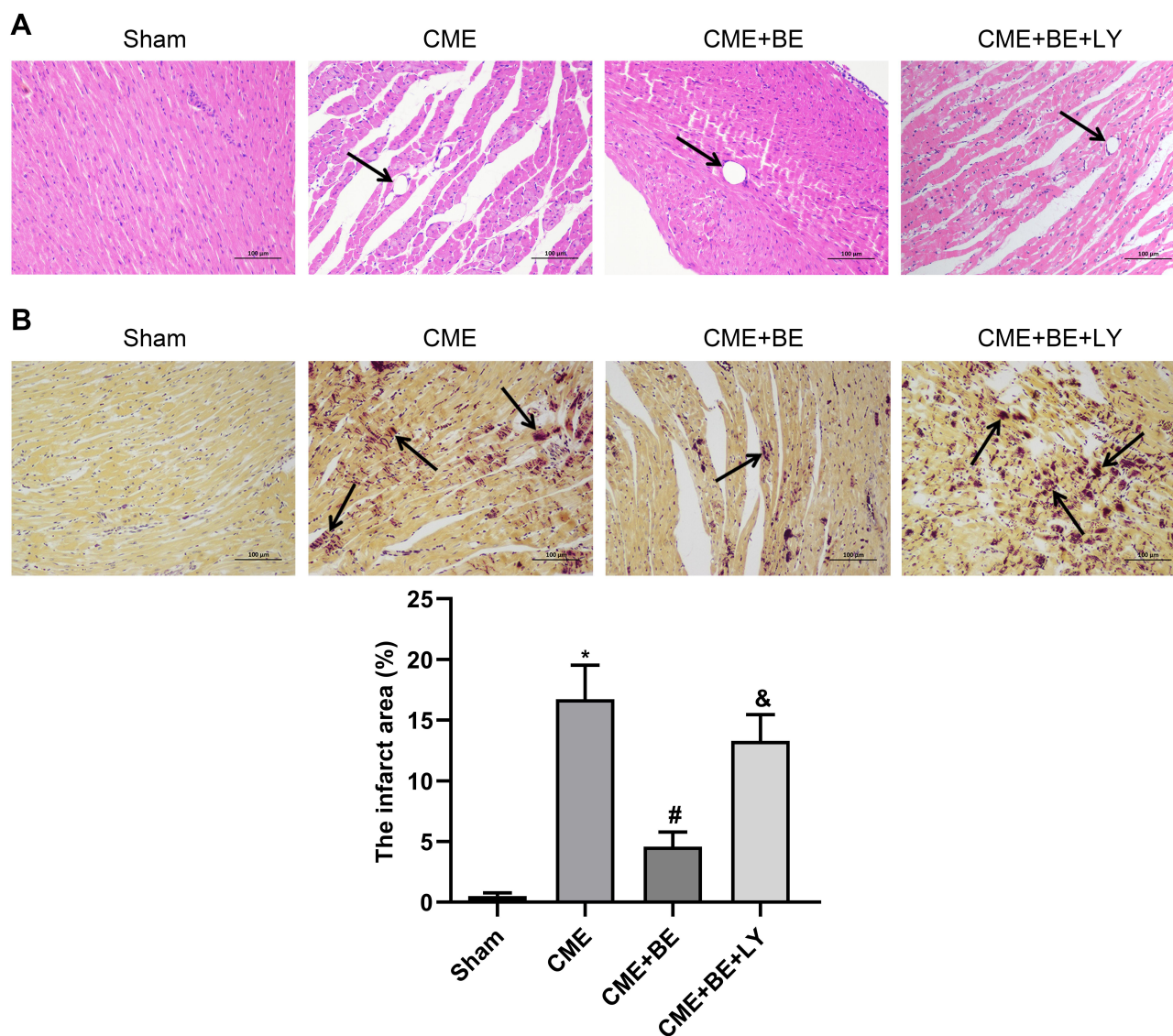


Figure 3 Histopathological examination of myocardial tissues through HE and HBF staining ($\times 200$ magnification; bar = 100 μm) ($n = 3$ for each group). **(A)** HE staining. Microspheres with inflammatory cell infiltration were observed in the CME, CME+BE and CME + BE + LY groups but not in the sham category. The arrows indicate the microspheres. **(B)** HBF staining. An ischemic myocardium is highlighted in red. The arrows indicate the microinfarct area. Data are presented as the mean \pm standard deviation (SD). * $P < 0.05$ versus the sham group; # $P < 0.05$ versus the CME group; & $P < 0.05$ versus the CME + BE group.

Abbreviations: CME, coronary microembolization; BE, breviscapine; LY, LY294002.

the regions of microinfarction caused by CME, with cytoplasmic red staining and degeneration. Moreover, the results revealed peripheral myocardial edema, erythrocyte exudation, peripheral inflammatory cell infiltration and microembolism in the arteriole. Notably, administration of breviscapine was shown to significantly alleviate the above conditions, reducing both peripheral myocardial edema and inflammatory cell infiltration. However, treatment with a combination of breviscapine and LY294002 significantly reversed these beneficial effects. Additionally, HBF staining demonstrated that the microinfarct lesions were mostly wedge-shaped, locally distributed and

nontransmural. They were also mostly located in the sub-endocardium and the left ventricle. Moreover, the infarct sizes in the sham, CME, CME + BE and CME + BE + LY groups were $0.52 \pm 0.25\%$, $16.72 \pm 2.81\%$, $4.57 \pm 1.20\%$ and $13.28 \pm 2.17\%$, respectively. Compared to the CME group, there was a significant decrease in the infarct size of the CME + BE group ($P < 0.05$), indicating that pretreatment with breviscapine might have inhibited the myocardial microinfarct area after CME induction in rats. However, treatment with a combination of breviscapine and LY294002 eliminated the effect of breviscapine on the myocardial microinfarct area.

Breviscapine Attenuated Cardiomyocyte Apoptosis After CME

The study further used TUNEL staining to assess apoptosis in cardiomyocytes (Figure 4). The normal nuclei appeared light blue while the apoptotic ones stained yellow-brown (TUNEL positive). Notably, myocardial apoptosis in rats in the sham group was occasionally recorded in papillary muscles and the subendocardium. In contrast, the number of TUNEL-positive cells increased significantly in the CME group ($P < 0.05$) compared to the sham category. Additionally, these apoptotic cardiomyocytes were primarily located in the myocardial micro-infarct and peri-infarct regions following CME induction. Moreover, there was a considerable decrease in TUNEL positive cells in the micro-infarct and peri-infarct zones of rats in the CME + BE group compared to those in the CME category ($P < 0.05$). However, treatment with a combination of breviscapine and LY294002 reversed the anti-apoptotic effect of breviscapine. Furthermore, the myocardial apoptotic index in the sham, CME, CME + BE and CME + BE + LY groups was $3.34 \pm 1.46\%$, $32.93 \pm 8.11\%$, $11.61 \pm 0.91\%$ and $31.51 \pm 4.75\%$, respectively.

Pretreatment with Breviscapine Attenuated CME-Induced Myocardial Inflammation

The study used qRT-PCR and Western blot analysis to examine the mRNA and protein expression levels of TNF- α and IL-1 β in the myocardium of rats, to confirm the presence of myocardial inflammation after CME induction (Figure 5A and B). The findings revealed that the mRNA and protein expression levels of TNF- α and IL-1 β were significantly higher in the CME group compared to the sham category ($P < 0.05$). On the other hand, the mRNA and protein expression levels of TNF- α and IL-1 β were substantially lower in the CME+BE group compared to the CME category ($P < 0.05$). Interestingly, the effect of breviscapine on the levels of TNF- α and IL-1 β was cancelled following co-treatment with LY294002.

Pretreatment with Breviscapine Attenuated CME-Induced Myocardial Apoptosis

Herein, the study evaluated the expression of cleaved caspase-3, Bax and Bcl-2 in the myocardium of rats in each group through qRT-PCR and Western blot analysis, to

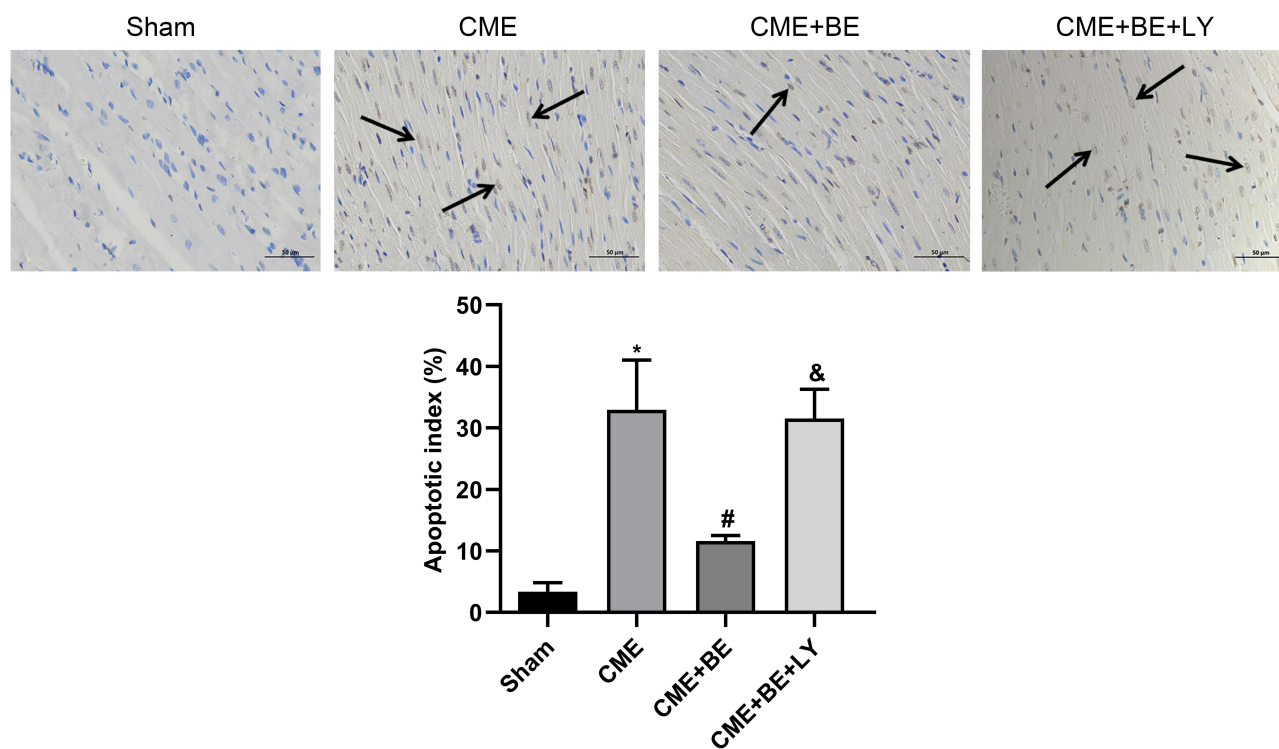


Figure 4 Detection of myocardial apoptosis through TUNEL staining ($\times 400$ magnification; bar = 50 μm) ($n = 3$ for each group). Normal nuclei were stained light blue while the nuclei of apoptotic cardiomyocytes were stained yellow-brown. Arrows indicate the nuclei of apoptotic cardiomyocytes. Data are presented as the mean \pm standard deviation (SD). * $P < 0.05$ versus the sham group; # $P < 0.05$ versus the CME group; & $P < 0.05$ versus the CME + BE group.

Abbreviations: CME, coronary microembolization; BE, breviscapine; LY, LY294002.

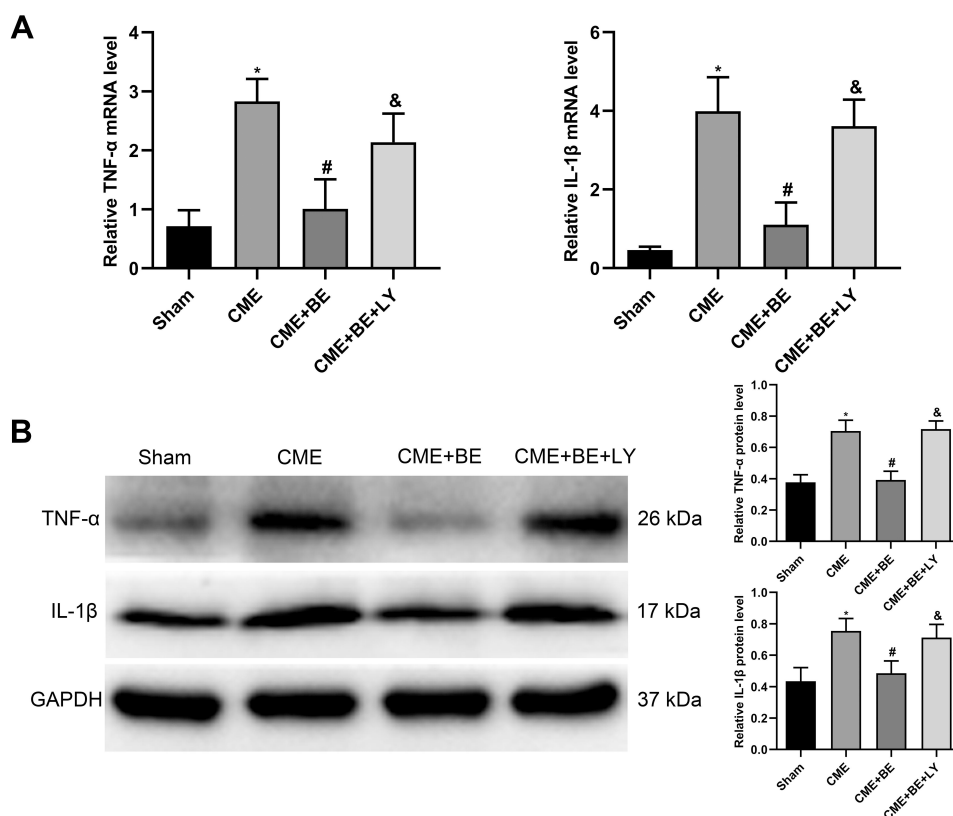


Figure 5 Pretreatment with breviscapine attenuated CME-induced myocardial inflammation (n = 4 for each group). **(A)** The mRNA expression levels of TNF- α and IL-1 β in cardiac tissues. **(B)** The protein expression levels of TNF- α and IL-1 β in cardiac tissues. Data are presented as the mean \pm standard deviation (SD). * $P < 0.05$ versus the sham group; # $P < 0.05$ versus the CME group; & $P < 0.05$ versus the CME + BE group.

Abbreviations: CME, coronary microembolization; BE, breviscapine; LY, LY294002.

verify the presence of cardiomyocyte apoptosis following CME (Figure 6A and B). Compared to the sham category, the results showed that the mRNA and protein expression levels of Bax and cleaved caspase-3 were significantly increased in the CME group, while the mRNA and protein expression levels of Bcl-2 were distinctly decreased ($P < 0.05$).

In addition, the mRNA and protein expression levels of Bax and cleaved caspase-3 in the CME+BE group were markedly decreased, whereas the mRNA and protein expression levels of Bcl-2 were significantly increased ($P < 0.05$), compared to the CME category. Nonetheless, the effect of breviscapine on the expression levels of Bax, cleaved caspase-3 and Bcl-2 was reversed following co-treatment with LY294002. Moreover, the IHC results from myocardial tissues (Figure 6C) were consistent with those from qRT-PCR and Western blotting. In general, these results indicated that pretreatment with breviscapine could effectively reduce CME-induced apoptosis in cardiomyocytes.

Inhibition of Myocardial Inflammation and Apoptosis by Breviscapine Involved the PI3K/Akt/GSK-3 β Signaling Pathway

The results from Western blot analysis revealed no significant differences in total PI3K, total Akt and total GSK-3 β among the four groups (Figure 7). Interestingly, myocardial expression of p-PI3K, p-Akt and p-GSK-3 β was significantly down-regulated in the CME group, compared to the sham category ($P < 0.05$). On the other hand, myocardial expression of p-PI3K, p-Akt and p-GSK-3 β was dramatically up-regulated ($P < 0.05$) in the CME+BE group compared to the CME category. However, the effect of breviscapine on the expression levels of p-PI3K, p-Akt and p-GSK-3 β was reversed upon co-treatment with LY294002. Collectively, these findings suggested that pretreatment with breviscapine could effectively attenuate myocardial inflammation and apoptosis following CME and this was closely associated with activation of the PI3K/Akt/GSK-3 β signaling pathway.

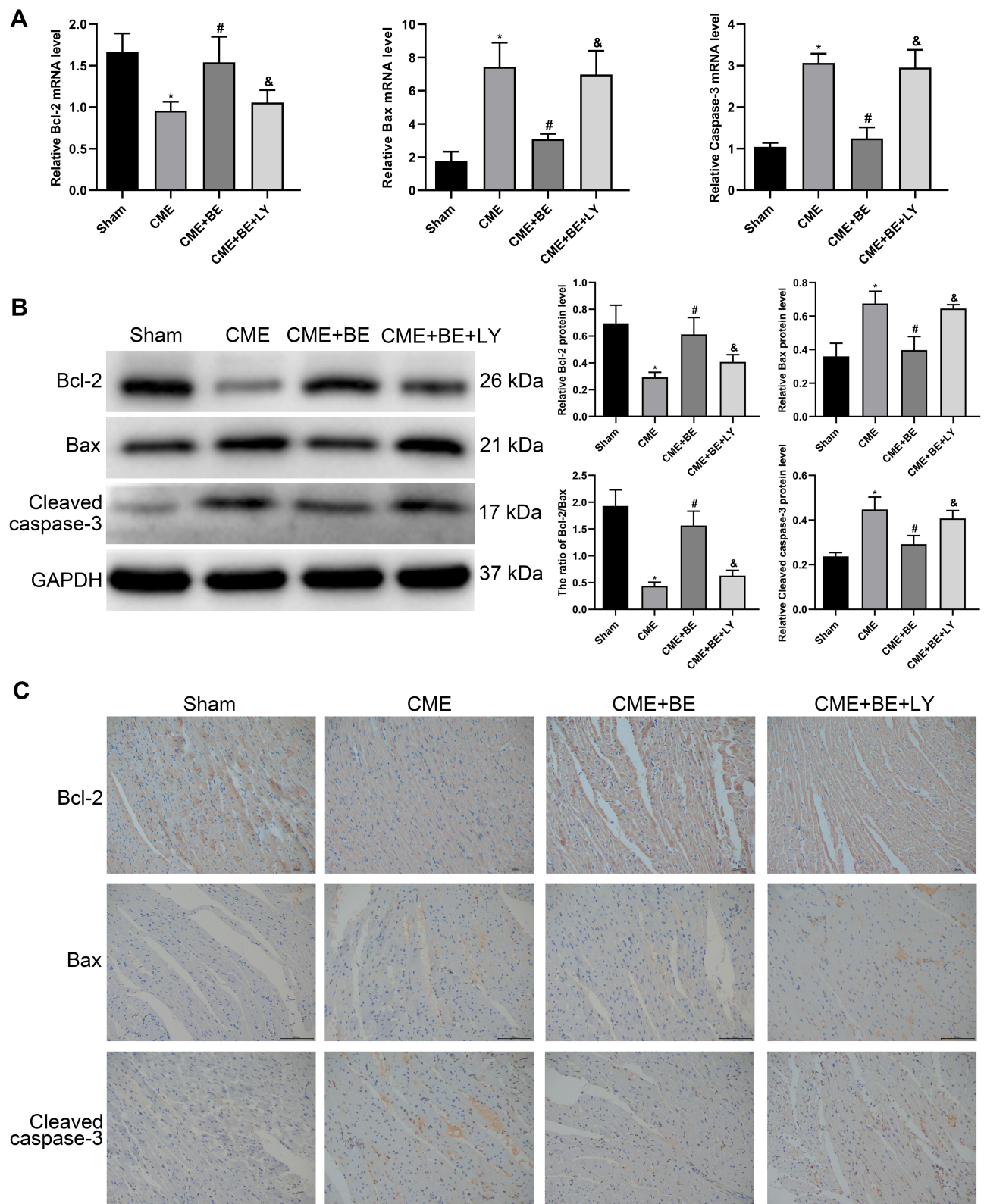


Figure 6 Pretreatment with breviscapine attenuated CME-induced myocardial apoptosis ($n = 4$ for each group). **(A)** The mRNA expression levels of Bcl-2, Bax and cleaved caspase-3 in cardiac tissues. **(B)** The protein expression levels of Bcl-2, Bax and cleaved caspase-3 in cardiac tissues. **(C)** Representative immunohistochemical pictures of Bcl-2, Bax and cleaved caspase-3 in cardiac tissues ($\times 200$ magnification; bar = 100 μm). Data are presented as the mean \pm standard deviation (SD). * $P < 0.05$ versus the sham group; # $P < 0.05$ versus the CME group; & $P < 0.05$ versus the CME + BE group.

Abbreviations: CME, coronary microembolization; BE, breviscapine; LY, LY294002.

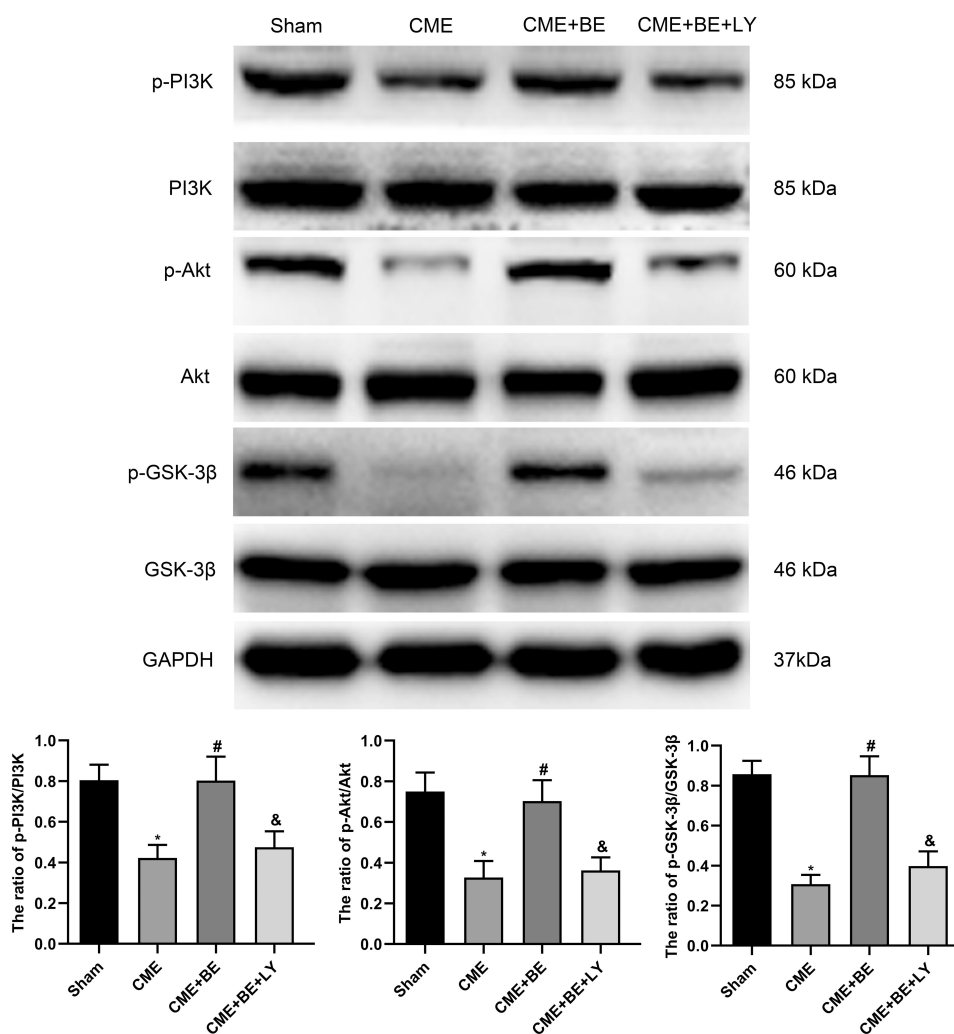


Figure 7 Effect of breviscapine on PI3K/Akt/GSK-3 β -associated protein expression in cardiac tissues (n = 4 for each group). Data are presented as the mean \pm standard deviation (SD). * P < 0.05 versus the sham group; # P < 0.05 versus the CME group; & P < 0.05 versus the CME + BE group.

Abbreviations: CME, coronary microembolization; BE, breviscapine; LY, LY294002.

Discussion

The present study uncovered a number of novel findings. First, the results revealed that myocardial inflammation and apoptosis were crucial factors in myocardial injury and cardiac dysfunction in rats following CME modelling. The results also showed that the PI3K/Akt/GSK-3 β signaling pathway had an important effect on CME-induced myocardial inflammation and apoptosis. Second, the study showed that pretreatment with breviscapine, seven days before CME induction, could effectively suppress myocardial inflammation and apoptosis, thus inhibiting myocardial injury. And as far as we know, this is the first study to simultaneously investigate the effects of breviscapine on myocardial inflammation and apoptosis in the same animal model of cardiovascular disease. Third, the

underlying protective mechanism of breviscapine in CME-related myocardial injury was significantly related to activation of the PI3K/Akt/GSK-3 β signaling pathway. Overall, these results emphasized on the significant effect of the PI3K/Akt/GSK-3 β pathway in the pathogenesis of CME-induced myocardial inflammation and apoptosis. Furthermore, this study for the first time showed that breviscapine may inhibit myocardial inflammation and apoptosis following CME by regulating the PI3K/Akt/GSK-3 β pathway, thereby improving CME-related cardiac dysfunction and reducing myocardial injury. Therefore, pretreatment with breviscapine holds potential for the management of CME-induced myocardial injury.

Notably, CME occurs spontaneously in patients with atherosclerotic plaque rupture or erosion and acute

coronary syndrome during PCI, which is a serious and complex condition.²⁰ In addition, CME-induced left ventricular dysfunction differs from the obstruction of the epicardial proximal coronary artery and also has no close relationship with the degree of myocardial perfusion defect,²¹ and can neither be explained by microinfarction nor insufficiency in local myocardial perfusion. However, myocardial apoptosis and inflammation were shown to play an essential role in myocardial injury and progressive cardiac dysfunction following CME in typical myocardial tissue around the microinfarct area. Therefore, inhibition of myocardial apoptosis and inflammation can greatly improve CME-induced cardiac dysfunction.^{22,23} In this study, the results revealed that rats in the CME model had worse myocardial apoptosis and inflammation compared to those in the sham group. The cardiac function of rats in the CME model was also shown to deteriorate, corresponding to the pathological changes in CME.

Breviscapine is an active ingredient of flavonoid glycosides extracted from *Erigeron breviscapus*.²⁴ The drug was shown to inhibit platelet aggregation, scavenge free oxygen radicals, reduce vascular resistance, dilate blood vessels and improve microcirculation.^{25–27} Additionally, it can potentially be applied in both cardiovascular and cerebrovascular diseases due to its comprehensive pharmacological effects, diverse mechanisms and high levels of safety.²⁸ Moreover, a previous study showed that treatment with breviscapine could down-regulate the levels inflammatory cytokines including TNF- α , IL-6 and IL-1 β as well as the monocyte chemoattractant protein (MCP)-1 in a CCl₄-induced acute liver injury model of C57BL/6 mice, thus inhibiting inflammation. On the other hand, it was shown to increase the expression of Bcl-2 and distinctly decreased the levels of Bax, active caspase-3 and poly (ADP ribose) polymerase (PARP), hence reducing apoptosis. Furthermore, breviscapine can block CCl₄-induced oxidative stress by increasing superoxide dismutase (SOD) activity and reducing the levels of malondialdehyde (MDA), consequently impeding mitogen-activated protein kinase pathways.²⁹ In addition, Bao et al suggested that breviscapine can effectively inhibit hepatocyte apoptosis by blocking the mitochondrial-dependent apoptosis pathway, in a rat hepatic ischemia/reperfusion injury model. This is primarily achieved by promoting the expression of mitofusin 2 and inhibiting the release of mitochondrial cytochrome c and decreasing the levels of cleaved caspase-3 protein.³⁰ Moreover, breviscapine displayed a dose-related anti-apoptotic effect in a transient focal cerebral ischemia model of rats.³¹ An

additional study by Li et al¹¹ also revealed that pretreatment with breviscapine could significantly reduce intracellular levels of free Ca²⁺, LDH leakage, apoptosis and necrosis in cardiomyocytes subjected to hypoxia, therefore exerting protective effects on the myocardium. Additionally, Wang et al reported that treatment with breviscapine could decrease the levels of active caspase-3 and up-regulate Bcl-2 by activating the PI3K/Akt/eNOS pathway. This effectively inhibited cardiomyocyte apoptosis induced by myocardial ischemia/reperfusion in vivo and simulated ischemia/reperfusion in vitro.¹⁴ In summary, the above background coupled the findings from the present study suggest that pretreatment with breviscapine may alleviate CME-induced myocardial inflammation and apoptosis by regulating the PI3K/Akt signaling pathway.

Additionally, various studies confirmed that the PI3K/Akt signaling pathway is critical in CME-induced myocardial injury and is also a common signaling pathway used by multiple drugs to facilitate cardioprotection.^{32,33} In addition, several effector proteins and intracellular mediators of signal transduction are involved in the PI3K/Akt signaling pathway. More specifically, GSK-3 β is considered a downstream target for this signaling pathway.³⁴ Notably, recent studies uncovered a variety of factors regulating the cell survival phosphorylate GSK-3 β by effectively activating the PI3K/Akt pathway, hence suppressing the biological activity of the GSK-3 β protein, eventually promoting cell survival.^{35,36} Moreover, numerous studies confirmed that the PI3K/Akt/GSK-3 β -dependent signaling pathway may be one of the most important and indispensable endogenous negative feedback mechanisms in the cell and produces a compensatory response under harmful stimuli, to inhibit cell apoptosis and inflammatory events.^{37,38} Furthermore, previous studies revealed that activation of the PI3K/Akt/GSK-3 β pathway distinctly attenuates myocardial inflammation, apoptosis and myocardial injury although it may have opposite biological effects when it is inactivated.^{39,40} And one mechanism by which PI3K/Akt signaling pathway regulates apoptosis via Bcl-2 is that the expression of Bcl-2 is up-regulated when the PI3K/Akt pathway is activated, and over-expression of Bcl-2 can inhibit the release of cytochrome C in the mitochondria and form a stable Bcl-2/Bax heterodimer with bax, thereby inhibiting Bax-induced apoptosis. Conversely, apoptosis is promoted when the expression of Bax is increased.⁴¹ In this study, the results demonstrated that pretreatment with breviscapine distinctively increased the expression levels of

p-PI3K, p-Akt, p-GSK-3 β and Bcl-2 after inducing CME in rats. However, breviscapine significantly reduced the levels of TNF- α , IL-1 β , Bax and cleaved caspase-3. Nonetheless, co-treatment with LY294002 (a specific inhibitor of PI3K) significantly reversed the protective effects exerted by breviscapine. Moreover, the findings in this study showed a decrease in cardiac function after inhibition of the PI3K/Akt signaling pathway but an increase in serum cTnI levels, microinfarct size and myocardial apoptosis, indicating that LY294002 could reverse the cardioprotective effects of breviscapine. Generally, these findings suggested that the PI3K/Akt/GSK-3 β pathway was closely associated with the protective effects of breviscapine in CME-induced myocardial injury. Therefore, it is highly possible that breviscapine can exert a cardioprotective effect by activating the PI3K/Akt/GSK-3 β pathway, thus inhibiting myocardial inflammation and apoptosis.

This research has some limitations. First, we established a CME rat model by injecting physical microembolic spheres into the coronary microvessels. However, this type of plastic microspheres has no biological properties such as thrombotic activity, vascular activity, or inflammatory tendency, so the pathophysiological changes of CME model caused by this plastic material are different from those caused by atherosclerotic plaque in clinic. Second, based on the pretreatment with breviscapine and the application of PI3K specific inhibitor LY294002, this study explored the effect of breviscapine on CME-induced myocardial inflammation and apoptosis and its regulatory effect on PI3K/Akt/GSK-3 β signaling pathway. However, the application of inhibitors or agonists of PI3K downstream molecules is very necessary to further explore the specific regulatory mechanism of breviscapine on the PI3K/Akt/GSK-3 β pathway in CME. Third, the molecular mechanisms involved in the regulation of inflammation and apoptosis are very complex, and it cannot be ruled out whether there are other potential signaling pathways participating in CME-induced myocardial injury, which needs further research.

In conclusion, this study demonstrated that breviscapine exerts an important cardioprotective effect in myocardial injury caused by CME, probably by activating the PI3K/Akt/GSK-3 β signaling pathway, hence distinctly attenuating myocardial inflammation and apoptosis. Therefore, breviscapine holds potential for use in the prevention and clinical therapy of CME-induced myocardial injury.

Acknowledgments

This study was supported by the National Natural Science Foundation of China (Grant No.81770346) and the Project for Innovative Research Team in Guangxi Natural Science Foundation (Grant No.2018GXNSFGA281006).

Disclosure

The authors declare no conflicts of interest in this work.

References

1. Heusch G, Skyschally A, Kleinbongard P. Coronary microembolization and microvascular dysfunction. *Int J Cardiol.* 2018;258:17–23. doi:10.1016/j.ijcard.2018.02.010
2. Otto S, Seeber M, Fujita B, et al. Microembolization and myonecrosis during elective percutaneous coronary interventions in diabetic patients: an intracoronary doppler ultrasound study with 2-year clinical follow-up. *Basic Res Cardiol.* 2012;107(5):289. doi:10.1007/s00395-012-0289-x
3. Liu Y, Liu Y, Huang X, Zhang J, Yang L. Protective effects and mechanism of curcumin on myocardial injury induced by coronary microembolization. *J Cell Biochem.* 2019;120(4):5695–5703. doi:10.1002/jcb.27854
4. Wang JY, Chen H, Su X, Zhou Y, Li L. Atorvastatin pretreatment inhibits myocardial inflammation and apoptosis in swine after coronary microembolization. *J Cardiovasc Pharmacol Ther.* 2017;22(2):189–195. doi:10.1177/1074248416662348
5. Liang J, Li L, Sun Y, He W, Wang X, Su Q. The protective effect of activating Nrf2/HO-1 signaling pathway on cardiomyocyte apoptosis after coronary microembolization in rats. *BMC Cardiovasc Disord.* 2017;17(1):272. doi:10.1186/s12872-017-0704-1
6. Kong B, Qin Z, Ye Z, Yang X, Li L, Su Q. microRNA-26a-5p affects myocardial injury induced by coronary microembolization by modulating HMGA1. *J Cell Biochem.* 2019;120(6):10756–10766. doi:10.1002/jcb.28367
7. Su Q, Lv X, Ye Z. Ligustrazine attenuates myocardial injury induced by coronary microembolization in rats by activating the PI3K/Akt pathway. *Oxid Med Cell Longev.* 2019;2019:6791457. doi:10.1155/2019/6791457
8. Gao J, Chen G, He H, et al. Therapeutic effects of breviscapine in cardiovascular diseases: a review. *Front Pharmacol.* 2017;8:289. doi:10.3389/fphar.2017.00289
9. Yan L, Huang H, Tang QZ, et al. Breviscapine protects against cardiac hypertrophy through blocking PKC- α -dependent signaling. *J Cell Biochem.* 2010;109(6):1158–1171. doi:10.1002/jcb.22495
10. Jia JH, Chen KP, Chen SX, Liu KZ, Fan TL, Chen YC. Breviscapine, a traditional Chinese medicine, alleviates myocardial ischaemia reperfusion injury in diabetic rats. *Acta Cardiol.* 2008;63(6):757–762. doi:10.2143/AC.63.6.2033394
11. Li XL, Li YQ, Yan WM, et al. A study of the cardioprotective effect of breviscapine during hypoxia of cardiomyocytes. *Planta Med.* 2004;70(11):1039–1044. doi:10.1055/s-2004-832644
12. Wang M, Zhang WB, Song JL, Luan Y, Jin CY. Effect of breviscapine on recovery of viable myocardium and left ventricular remodeling in chronic total occlusion patients after revascularization: rationale and design for a randomized controlled trial. *Med Sci Monit.* 2018;24:4602–4609. doi:10.12659/MSM.906438
13. Zhang H, Song Y, Li Z, Zhang T, Zeng L. Evaluation of breviscapine on prevention of experimentally induced abdominal adhesions in rats. *Am J Surg.* 2016;211(6):1143–1152. doi:10.1016/j.amjsurg.2015.05.037
14. Wang J, Ji SY, Liu SZ, Jing R, Lou WJ. Cardioprotective effect of breviscapine: inhibition of apoptosis in H9c2 cardiomyocytes via the PI3K/Akt/eNOS pathway following simulated ischemia/reperfusion injury. *Die Pharmazie.* 2015;70(9):593–597.

15. Zhong D, Yang B, Chen X, Li K, Xu J. Determination of scutellarin in rat plasma by high-performance liquid chromatography with ultra-violet detection. *J Chromatogr B Analyt Technol Biomed Life Sci*. 2003;796(2):439–444. doi:10.1016/j.jchromb.2003.08.002
16. Mao Q, Liang X, Wu Y, Lu Y. Resveratrol attenuates cardiomyocyte apoptosis in rats induced by coronary microembolization through SIRT1-mediated deacetylation of p53. *J Cardiovasc Pharmacol Ther*. 2019;24(6):551–558. doi:10.1177/1074248419845916
17. Su Q, Lv X, Sun Y, Ye Z, Kong B, Qin Z. Role of TLR4/MyD88/NF-kappaB signaling pathway in coronary microembolization-induced myocardial injury prevented and treated with nicorandil. *Biomed Pharmacother*. 2018;106:776–784. doi:10.1016/j.biopha.2018.07.014
18. Zhu HH, Wang XT, Sun YH, et al. MicroRNA-486-5p targeting PTEN protects against coronary microembolization-induced cardiomyocyte apoptosis in rats by activating the PI3K/AKT pathway. *Eur J Pharmacol*. 2019;855:244–251. doi:10.1016/j.ejphar.2019.03.045
19. Chen QF, Wang W, Huang Z, et al. Role of high-mobility group B1 in myocardial injury induced by coronary microembolization in rats. *J Cell Biochem*. 2019;120(3):4238–4247. doi:10.1002/jcb.27709
20. Bose D, von Birgelen C, Zhou XY, et al. Impact of atherosclerotic plaque composition on coronary microembolization during percutaneous coronary interventions. *Basic Res Cardiol*. 2008;103(6):587–597. doi:10.1007/s00395-008-0745-9
21. Dorge H, Neumann T, Behrends M, et al. Perfusion-contraction mismatch with coronary microvascular obstruction: role of inflammation. *Am J Physiol Heart Circ Physiol*. 2000;279(6):H2587–H2592. doi:10.1152/ajpheart.2000.279.6.H2587
22. Sun YH, Su Q, Li L, Wang XT, Lu YX, Liang JB. Expression of p53 in myocardium following coronary microembolization in rats and its significance. *J Geriatr Cardiol*. 2017;14(5):292–300. doi:10.11909/j.issn.1671-5411.2017.05.007
23. Su Q, Lv X, Sun Y, Yang H, Ye Z, Li L. Role of high mobility group A1/nuclear factor-kappa B signaling in coronary microembolization-induced myocardial injury. *Biomed Pharmacother*. 2018;105:1164–1171. doi:10.1016/j.biopha.2018.06.098
24. Guan YB, Yang DR, Nong SJ, et al. Breviscapine (BVP) inhibits prostate cancer progression through damaging DNA by minichromosome maintenance protein-7 (MCM-7) modulation. *Biomed Pharmacother*. 2017;93:103–116. doi:10.1016/j.biopha.2017.06.024
25. Guo C, Zhu Y, Weng Y, et al. Therapeutic time window and underlying therapeutic mechanism of breviscapine injection against cerebral ischemia/reperfusion injury in rats. *J Ethnopharmacol*. 2014;151(1):660–666. doi:10.1016/j.jep.2013.11.026
26. Hong H, Liu GQ. Scutellarin attenuates oxidative glutamate toxicity in PC12 cells. *Planta Med*. 2004;70(5):427–431.
27. Wu L, Liu M, Fang Z. Combined therapy of hypertensive nephropathy with breviscapine injection and antihypertensive drugs: a systematic review and a meta-analysis. *Evid Based Complement Alternat Med*. 2018;2018:2958717. doi:10.1155/2018/2958717
28. Jiang L, Xia QJ, Dong XJ, et al. Neuroprotective effect of breviscapine on traumatic brain injury in rats associated with the inhibition of GSK3beta signaling pathway. *Brain Res*. 2017;1660:1–9. doi:10.1016/j.brainres.2017.01.031
29. Liu Y, Wen PH, Zhang XX, Dai Y, He Q. Breviscapine ameliorates CCl4-induced liver injury in mice through inhibiting inflammatory apoptotic response and ROS generation. *Int J Mol Med*. 2018;42(2):755–768. doi:10.3892/ijmm.2018.3651
30. Bao Z, Chen W, Pan F, Peng B, Gong J. Role of mitofusin 2 in the protective effect of breviscapine against hepatic ischemia/reperfusion injury in rats. *Exp Ther Med*. 2018;15(4):3582–3588. doi:10.3892/etm.2018.5834
31. Yiming L, Wei H, Aihua L, Fandian Z. Neuroprotective effects of breviscapine against apoptosis induced by transient focal cerebral ischaemia in rats. *J Pharm Pharmacol*. 2008;60(3):349–355. doi:10.1211/jpp.60.3.0010
32. Su Q, Li L, Zhao J, Sun Y, Yang H. Effects of nicorandil on PI3K/Akt signaling pathway and its anti-apoptotic mechanisms in coronary microembolization in rats. *Oncotarget*. 2017;8(59):99347–99358. doi:10.18632/oncotarget.19966
33. Mao Q, Liang X, Wu Y, Lu Y. Nobiletin protects against myocardial injury and myocardial apoptosis following coronary microembolization via activating PI3K/Akt pathway in rats. *Naunyn Schmiedebergs Arch Pharmacol*. 2019;392(9):1121–1130. doi:10.1007/s00210-019-01661-y
34. Kim SA, Kang OH, Kwon DY. Cryptotanshinone induces cell cycle arrest and apoptosis of NSCLC cells through the PI3K/Akt/GSK-3beta pathway. *Int J Mol Sci*. 2018;19(9). doi:10.3390/ijms19092739
35. Zhang X, Shi M, Ye R, et al. Ginsenoside Rd attenuates tau protein phosphorylation via the PI3K/AKT/GSK-3beta pathway after transient forebrain ischemia. *Neurochem Res*. 2014;39(7):1363–1373. doi:10.1007/s11064-014-1321-3
36. Park SJ, Jin ML, An HK, et al. Emodin induces neurite outgrowth through PI3K/Akt/GSK-3beta-mediated signaling pathways in Neuro2a cells. *Neurosci Lett*. 2015;588:101–107. doi:10.1016/j.neulet.2015.01.001
37. Zheng T, Yang X, Wu D, et al. Salidroside ameliorates insulin resistance through activation of a mitochondria-associated AMPK/PI3K/Akt/GSK3beta pathway. *Br J Pharmacol*. 2015;172(13):3284–3301. doi:10.1111/bph.13120
38. Zhang Y, Zhang Z, Wang H, et al. Neuroprotective effect of ginsenoside Rg1 prevents cognitive impairment induced by isoflurane anesthesia in aged rats via antioxidant, anti-inflammatory and anti-apoptotic effects mediated by the PI3K/AKT/GSK-3beta pathway. *Mol Med Rep*. 2016;14(3):2778–2784. doi:10.3892/mmr.2016.5556
39. Wei D, Xu H, Gai X, Jiang Y. Astragaloside IV alleviates myocardial ischemia-reperfusion injury in rats through regulating PI3K/AKT/GSK-3beta signaling pathways. *Acta Cir Bras*. 2019;34(7):e201900708. doi:10.1590/s0102-865020190070000008
40. Zhang L, Guo Z, Wang Y, Geng J, Han S. The protective effect of kaempferol on heart via the regulation of Nrf2, NF-kβ, and PI3K/Akt/GSK-3β signaling pathways in isoproterenol-induced heart failure in diabetic rats. *Drug Dev Res*. 2019;80(3):294–309. doi:10.1002/ddr.21495
41. Tsukahara S, Yamamoto S, Tin Tin Win S, et al. Inhalation of low-level formaldehyde increases the Bcl-2/Bax expression ratio in the hippocampus of immunologically sensitized mice. *Neuroimmunomodulation*. 2006;13(2):63–68. doi:10.1159/000094829

Drug Design, Development and Therapy

Publish your work in this journal

Drug Design, Development and Therapy is an international, peer-reviewed open-access journal that spans the spectrum of drug design and development through to clinical applications. Clinical outcomes, patient safety, and programs for the development and effective, safe, and sustained use of medicines are a feature of the journal, which has also

been accepted for indexing on PubMed Central. The manuscript management system is completely online and includes a very quick and fair peer-review system, which is all easy to use. Visit <http://www.dovepress.com/testimonials.php> to read real quotes from published authors.

Submit your manuscript here: <https://www.dovepress.com/drug-design-development-and-therapy-journal>

Dovepress